

Evaluating synthetic fuel production: A case study on the influence of electricity and CO₂ price variations

David Huber^{*}, Felix Birkelbach, René Hofmann

TU Wien, Institute of Energy Systems and Thermodynamics, Getreidemarkt 9/BA, 1060 Vienna, Austria

ARTICLE INFO

Keywords:

Sustainable fuel production
Synthetic fuels
Power-to-liquid
Optimization
Electricity and CO₂ price changes
Pareto front

ABSTRACT

To combat climate change, we need to reduce emissions from the transport sector. Synthetic fuels are a long-term solution for aviation, maritime and heavy machinery. Large-scale use requires cost-effectiveness, efficient production and resilience to price changes. In this case study, we simultaneously optimize the cell voltage of the solid oxide electrolysis cell, the heat exchanger network and the heat supply of a PtL-plant. PtL-efficiency and production costs are used as objectives to generate multiple Pareto fronts for future price scenarios. The results show that the sensitivity to price changes has different impacts on design and operating parameters, which can lead to unattractive solution domains in the Pareto front. Currently, synthetic fuels can be produced at 1.83–2.36 €/kg. In the best case, at 1.42–1.97 €/kg and 3.88–4.28 €/kg in the worst case. This paper supports decision-makers in planning PtL-plants to ensure sustainable synthetic fuel availability on a global scale.

1. Introduction

The leading causes of anthropogenic climate change are CO₂ emissions from the combustion of fossil fuels. The transport sector contributed with 7.95 Gt to approx. 21.60 % of the annual CO₂ emissions in 2022 [1,2]. Facing these figures, there is an increasing need to create a climate-neutral transport sector. Synthetic fuels from renewable energy sources and CO₂ offer a promising solution. They significantly reduce the carbon footprint from the transport sector since the combustion process only releases the CO₂ that was previously taken out of the atmosphere or has been emitted from another source, such as a cement plant [3]. Unlike fossil fuels, no previously bonded CO₂ is released into the atmosphere. Promising applications are conceivable both in the short term for existing passenger cars and in the long term for non-electrifiable sectors such as shipping, aviation and heavy machinery.

Several demonstration plants have been built in Europe in recent years [4]. These plants produce several thousand tons of methanol and Fischer–Tropsch (FT) fuels annually already. A list of currently operating plants and upcoming projects is provided by Pratschner et al. [5]. There is also an interactive map with additional sites in [6]. Another interesting map is the Power-to-X potential atlas by Fraunhofer IEE [7], which illustrates the enormous potential of synthetic fuel production sites. Nevertheless, so far little is known about the real production rates of synthetic fuels. The demonstration plant in Haru Oni, Chile, for example, produces fuel at costs of 50 €/L [8]. However, these costs are not representative for large-scale industrial production. They nevertheless reflect the problem of economically viable production. The production costs must be lowered to be financially relevant to end-users [9]. The analyses of Ueckerdt et al. [3] predict long-term production costs of less than 1 €/L. With production costs in the same order of magnitude as conventional fuels, synthetic fuels will be deployed. A detailed overview of the current production costs of synthetic fuels is given by Brynolf et al. [10].

^{*} Corresponding author.

E-mail address: david.huber@tuwien.ac.at (D. Huber).

<https://doi.org/10.1016/j.csite.2024.104975>

Received 13 March 2024; Received in revised form 5 August 2024; Accepted 13 August 2024

Available online 20 August 2024

2214-157X/© 2024 The Author(s). Published by Elsevier Ltd. This is an open access article under the CC BY-NC-ND license (<http://creativecommons.org/licenses/by-nc-nd/4.0/>).

Nomenclature

Acronyms

CAPEX	annual capital expenses
CS	combustion system
ETS	emission trading system
FT	Fischer–Tropsch
HEN	heat exchanger network
HENS	heat exchanger network synthesis
HEX	heat exchanger
IFE	Innovation Flüssige Energie, eng.: Innovation Liquid Energy
LCOP	levelized cost of product
LMTD	logarithmic mean temperature difference
MILP	mixed-integer linear programming
MIP	mixed-integer programming
MOO	multi objective optimization
OPEX	operational expenditures
PtG	power-to-gas
PtL	power-to-liquid
PtX	power-to-x
PV	photovoltaics
RMSE	root-mean-square error
RWGS	reverse water gas shift
SOEC	solid oxide electrolysis cell
TEA	techno-economic analyses

Superscripts

in	inlet
max	maximum
min	minimum
out	outlet

Subscripts

cu	cold utility
el	electric
hex	heat exchanger
hu	hot utility
prod	production
i	hot stream
j	cold stream
k	stage

Variables

β	cost exponent ()
ΔT_{\min}	minimum temperature difference (K)
\dot{H}	chemically bounded energy in FT-products (kW)
\dot{m}	mass flow (kg/h)
η_{PtL}	PtL-efficiency (%)
$CAPEX$	capital expenditures (€/y)
$CAPEX$	operating expenditures (€/y)
$LMTD$	logarithmic mean temperature difference (K)

TAC	total annual costs (€/y)
μ	dynamic viscosity (mPa/s)
ρ	density (kg m ³)
ε	coefficient of performance ()
a	depreciation period (y)
AF_{inv}	investment annualization factor (1/y)
AF_{op}	operational annualization factor ()
c_{el}	electricity costs (€/(MW h))
$c_{f,hex}$	step-fixed HEX costs (€/y)
c_{prod}	product costs (€/kg)
C_{sys}	investment costs (€)
$c_{v,hex}$	variable HEX costs (€/(m ² y))
c_f	feedstock costs (€/t)
F	flow capacity (kW/K)
h_{prod}	specific enthalpy of the product (MJ/kg)
N_{st}	number of stages
P_{el}	total electrical energy demand (kW)
P_{sys}	electrical energy demand w/o utilities (kW)
q	heat flow (kW)
T	temperature (°C)
t	annual full load hours (h/y)
U	overall heat transfer coefficient (kW/(m ² K))
U_{cell}	cell voltage (V)
z	binary variable for existence of HEX ()

The production costs of synthetic fuels are susceptible to various factors, which have been extensively analyzed in recent literature. Dahiru et al. [11] provide a comprehensive review of techno-economic analyses (TEAs) for power-to-X (PtX) technologies. The authors emphasize the importance of system efficiency, capital expenditures (CAPEX) and operational expenditures (OPEX) in calculating fuel production costs. The study underscores that efficiency improvements can reduce costs. The initial CAPEX and ongoing OPEX must be balanced for economic viability. For instance, Götz et al. [12] discuss how improving process efficiency in power-to-gas (PtG) systems may lead to crucial cost reductions, highlighting the role of technological advancements. Dieterich et al. [13] review Power-to-Liquid (PtL) pathways. They found that economies of scale and technological advancements can lower fuel production costs, reinforcing the importance of continued innovation in this field. Graves et al. [14] and Tremel et al. [15] explore the effects of using renewable energy sources. They found that the variability of electricity prices is a critical factor in the overall cost structure of synthetic fuels. The integration of CO₂ capture technologies, as discussed by Leeson et al. [16], adds another layer of complexity and cost sensitivity, given the significant expenses associated with capturing and utilizing CO₂ in synthetic fuel production. Other contributions include the works by Sternberg and Bardow [17] and Michailos et al. [18], which investigate the impact of feedstock prices and the efficiency of electrolysis processes on fuel production costs. They emphasize that fluctuations in feedstock prices, such as those for water and CO₂, alongside the efficiency of electrolysis, can considerably influence the economic feasibility of synthetic fuel production. The literature highlights that the sensitivity of fuel production costs to technological improvements, market conditions, and policy frameworks is a recurring theme. The research indicates that there is potential for reducing costs through technological innovation and economies of scale. However, the economic feasibility of synthetic fuels heavily relies on stable and low-cost renewable electricity, efficient CO₂ capture and utilization, and favorable policy environments.

The crucial challenges include producing fuels with competitive costs and in sufficient quantities. The production of synthetic fuels requires a complex interaction of processes, where various parameters, such as the operating point and heat integration, significantly impact costs and efficiency. Applying mathematical programming, the plant design, respectively, the interaction of sub-components can be optimized to meet defined objectives. However, optimizing only a constrained single objective problem may result in insufficient performance of other critical aspects compared to multi-criteria optimization (MOO) [19]. In this paper, the objectives PtL-efficiency and production costs are used.

The electricity price is another crucial factor that significantly impacts the production costs of synthetic fuels. Although production costs are not directly affected by CO₂ prices, the fuel price for end users is nevertheless affected. For the end users, the point at which the CO₂ prices are applied is not decisive since they are added to the fuel costs anyway. In this paper, we consider the CO₂ price as part of the production cost to ensure comparability with conventionally produced fuels. The prices for renewable electricity and CO₂ certificates can be subject to significant fluctuations due to technological leaps and changing policies. These fluctuations can have unforeseen effects on the economics of synthetic fuel costs. For the design optimization of the PtL-plant,

defined assumptions must be made for electricity and CO₂ prices. Changing prices after the commissioning of the plant can have unwanted effects on production costs. During the planning phase, it is essential to analyze the effects of price changes and consider their consequences when choosing the optimal plant design and operation.

1.1. Novelty & contribution

In this paper, we conduct a parametric study to understand the impact of changing electricity and CO₂ prices on the production costs of synthetic fuels. We perform an in-depth analysis based on the coupled optimization of the operating characteristics, the heat exchanger network (HEN) and the internal heat supply. PtL-efficiency and fuel production cost are used as objectives of the MOO problem. Starting from a Pareto front at current feedstock prices, the CO₂ and electricity prices are varied. We examine each cost parameter's sensitivity to operating and design characteristics and derive projected Pareto fronts within reasonable price scenarios. We show that fluctuating cost parameters affect design and operation parameters differently. Accordingly, the relevant region of the Pareto front can be narrowed and the plant can be designed to be more resilient. Our analyses are crucial to assess fuel production costs to changing market conditions and policies. This allows us to ensure that synthetic fuels can be made economically viable and available in sufficient quantities to meet global demand.

1.2. Paper organization

The novel 1 MW PtL-plant with its main components and characteristics is presented in Section 2.1. In Section 2.2, the methods for optimization, linearization and the transfer to MILP are presented. In Section 3.1 the modeling and the two antagonistic objectives, PtL-efficiency and production cost, are presented. Further, in Section 3.2 the correlation of the cost parameters with the objective functions and the parameter domain are described. In Section 4, the parameter study results and the cost parameters' sensitivities are analyzed and discussed.

2. Materials & methods

2.1. System description

In the context of the *IFE* (de.: Innovation Flüssige Energie, eng.: Innovation Liquid Energy) research project, a PtL-plant is designed to produce synthetic fuels using water, renewable electricity, exhaust gas from a cement plant and air as feedstock. The plant is designed with a maximum electrolysis capacity of approximately 1 MW using a high-temperature solid oxide co-electrolysis (co-SOEC). The PtL-plant is considered a stand-alone system. The waste heat generated is thus considered as a loss. However, integration into other industrial processes is conceivable depending on the location of the plant.

The selection of a 1 MW plant size was guided by the objective to thoroughly investigate the technical and economic feasibility of the proposed synthetic fuel production pathway on a smaller, pilot scale. This approach enables a comprehensive analysis of technological parameters and optimization strategies while effectively managing risk and investment. Although larger plants in the multi-MW range might benefit from improved economies of scale, the knowledge and insights obtained from this 1 MW plant are essential for informing the design and development of more economically viable large-scale systems in the future.

Fig. 1 shows a schematic of the process. Notably, the schematic does not include valves, pumps or compressors. For the sake of clarity, all heat transfer points are indicated with one-sided connected heat exchangers. This means that the heat exchangers are connected to each other based on the selected Pareto optimal solution in order to exchange heat. The resulting heat exchanger network is discussed in Section 4. The cold process streams are shown in blue, and the hot process streams are shown in red.

The PtL process is divided into the following five main components. A more detailed description of the process can be found in [20,21]. In particular, the correlations between the cell voltage of the co-SOEC and the power consumption, feedstock input, product output and efficiency are described in more detail.

Steam Generation Pure water at 20 °C is preheated, evaporated, and superheated in the steam generator.

CO₂ Conditioning The PtL-process utilizes exhaust gas from a cement plant with 15.17 wt% CO₂, 81.11 wt% N₂, and 3.72 wt% H₂O at 40 °C. The CO₂ is conditioned to a purity of 98.73 wt% with low residual water content through adsorption and desorption processes.

co-SOEC The central component is the co-SOEC, where conditioned CO₂ is superheated, mixed with superheated steam and reformed with preheated air to an H₂-rich gas and CO. The synthesis gas leaving the co-SOEC is cooled and condensed in four stages before entering the FT-reactor. With higher cell voltage, more feedstock is required and therefore the product output also increases. The composition of the synthesis gas remains almost unchanged.

FT-reactor and upgrading A catalytic conversion of the synthesis gas at high temperatures and pressure is carried out in the FT-reactor. The resulting syncrude is separated into FT-wax, diesel and naphtha and upgraded for final use. The product properties downstream of the separation are given in Appendix A. Unreacted synthesis gas is partially recirculated and fed into the combustion system.

Combustion System The combustion system (CS) comprises three serially connected combustion chambers. Unreacted synthesis gas from the separation is used as fuel gas. The CS serves as an internal hot utility to heat the cold process streams.

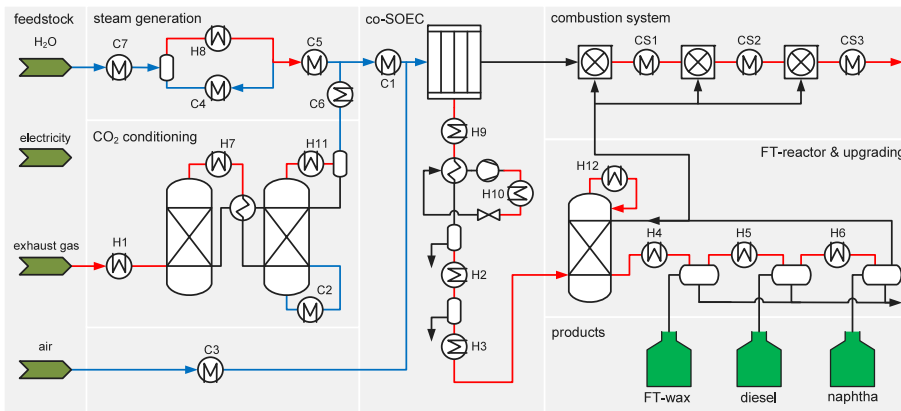


Fig. 1. Schematic representation of the 1 MW PtL-plant with the five main components and the heat exchangers.
Source: Adapted from [20].

2.2. Methods

The operating point of the co-SOEC influences the stream parameters inlet, outlet temperature and heat capacity flow of the HEN and vice versa; a holistic optimum can only be achieved by coupling operation and design optimization. The optimization performed in this paper is based on the extension of the classical heat exchanger network synthesis (HENS) by Huber et al. [20,22]. This formulation is based on the classic formulation by Yee & Grossman [23]. Contrary to the publications from Huber et al. this paper does not focus on the development of a holistic optimization approach that optimizes design and operation simultaneously. Rather, it builds on the existing approach and examines the influence of cost parameters and the effects on the Pareto front.

As an alternative to this deterministic formulation, genetic algorithms, which were presented for example by Lewin et al. [24], Luo et al. [25] and Stampfli et al. [26], are also conceivable options for solving a HENS problem. Compared to optimization with stochastic methods, the risk of getting stuck in a local optimum can be reduced by using mixed integer linear programming (MILP).

The HENS of Yee & Grossman [23] has been adapted to implement streams with variable temperatures and heat flow capacities. Furthermore, the formulation has been extended to include operating characteristics in the optimization problem. A fundamental assumption for this is that distinct operating points affect only the stream parameters and the objectives. For each operating variable, a piece-wise linear model is created to represent the interaction between the operating point and the stream parameters. For further information regarding the coupled optimization, we refer to [20].

In the case of the PtL-plant, the costs for CO₂ and electricity significantly influence the production costs. Therefore, the multi-criteria optimization problem is solved in the first instance, considering today's electricity and CO₂ costs. Based on the resulting non-dominated solutions, the cost parameters are varied to study their impact on PtL-efficiency and production costs. The domain in which the parameters vary is specified, considering future development scenarios with rising and falling prices. In a subsequent step, the objectives are recalculated with modified cost parameters for the given design and operating points of the non-dominated solutions. If objectives are recalculated with different parameters while the variables remain the same, this usually does not lead to optimal results. The choice of parameters affects the solution space of the optimization problem, so optimality cannot be guaranteed. In any case, optimality can be achieved by resolving the optimization problem. However, the objective functions cost parameters we vary do not require re-solving the optimization problems. This remarkably efficient approach is possible because the cost parameters do not directly affect the PtL-efficiency and only linearly affect the production costs. As a result, the non-dominated solutions of the Pareto front are only linearly shifted by the production costs at constant efficiency. This procedure enables us to highly efficiently assess the influence of different price scenarios on the system performance and production costs without performing time-consuming optimizations.

2.2.1. Multi-criteria optimization

In this paper, we use the epsilon constraint method to obtain uniformly distributed solutions on the Pareto front. However, the conventional epsilon constraint method is not able to find solutions in overhanging regions of the Pareto front. To overcome this shortcoming, a double-sided epsilon constraint method [22] is used. Therefore, both sides of the Pareto front are constrained to force the objective into a defined domain.

2.2.2. Linearization & transfer to MILP

Within the adapted HENS, piece-wise linear approximations are used to model all non-linearities. Both piece-wise convex combinations and plane simplices are used to model the multi-dimensional correlations for HEX areas, energy balances and objectives.

To expedite computation, piece-wise linear approximated functions are transformed into MILP with a minimal amount of binary variables. One-dimensional, mainly convex curved functions are converted to MILP without binary variables, while other functions necessitate binary variables. Employing the logarithmic coding approach, as proposed by Vielma and Nemhauser [27], minimizes the number of binary variables.

Additional information on the methods applied regarding the piece-wise linear approximation and the conversion to MILP can be found in [22].

3. Modeling

The modeling of the system is based on steady-state simulations with Aspen HYSIS. The use of Aspen HYSIS provides the ability to model complex chemical processes, including reactions, separation processes and heat exchange. This is supported by the extensive database and the use of accurate thermodynamic models that allow accurate representation of process conditions and outcomes. In addition, Aspen HYSIS offers flexibility in modeling so that different process variants and configurations can be investigated. This flexibility makes it possible to simulate different cell voltages of the co-SOEC as a main operating parameter and evaluate their effects on the overall process. The system was simulated for seven equidistant cell voltages between $U_{\text{cell}}^{\min} = 1.275 \text{ V}$ and $U_{\text{cell}}^{\max} = 1.305 \text{ V}$. The simulation data is used to model the system. Feedstock, power consumption of the co-SOEC, product output, and stream data for the HENS are modeled as a function of cell voltage. The systems' subcomponents' size is independent of the cell voltage, resulting in identical system costs. The size of the CS providing the internal heat is also independent of the cell voltage. Only the available amount of FT-offgas is limited depending on the cell voltage.

The simulations are based on steady-state assumptions, which means that time-dependent effects and dynamic behavior of the process are not taken into account. In addition, the model assumptions and simplifications, such as assumptions about ideal mixtures and no heat capacity changes with temperature, require a certain degree of caution, as they can lead to deviations from the real process conditions.

Detailed information on system modeling can be found in [20]. The parameters used to specify the streams and the heat exchanger network are given in Appendix B.

3.1. Objectives

Multi-objective optimization enables a holistic performance evaluation of the PtL-plant. In this paper, the antagonistic objectives PtL-efficiency and fuel production costs are optimized.

3.1.1. PtL-efficiency

Maximizing PtL-efficiency is crucial for reducing energy consumption in the production of synthetic fuels. Higher efficiency enables more effective use of renewable energy sources while also minimizing the need for resources such as land and raw materials.

The PtL-efficiency is maximized and described as the ratio of chemically bounded energy in the product \dot{H}_{prod} to electrical energy input P_{el} according to Eq. (1).

$$\max \eta_{\text{PtL}} = \frac{\dot{H}_{\text{prod}}}{P_{\text{el}}} = \frac{\sum_v \dot{m}_{\text{prod},v} h_{\text{prod},v}}{P_{\text{sys}} + \sum_j \epsilon_{\text{hu}} q_{\text{hu},j} + \sum_i \epsilon_{\text{cu}} q_{\text{cu},i}} \quad (1)$$

The chemically bonded energy downstream of the separation is derived from the sum of the product mass flow rates and the specific enthalpies.

A significant part of the total electrical energy demand P_{el} is the system power P_{sys} . With P_{sys} , the electric demand of the co-SOEC, circulation pumps, valves and control equipment and losses are covered. The two sums in the denominator represent the energy demand of the electrified utilities. A coefficient of performance of $\epsilon_{\text{cu}} = 0.05$ is assumed for the cold utilities. For the hot utilities, ϵ_{hu} is assumed to be 1.05.

3.1.2. Fuel production costs

The fuel production costs c_{prod} are minimized and modeled according to Eq. (2) as the ratio of total annual costs TAC to total synthetic fuel output $\sum_v t \dot{m}_{\text{prod},v}$.

$$\min c_{\text{prod}} = \frac{TAC}{\sum_v t \dot{m}_{\text{prod},v}} = \frac{CAPEX + OPEX}{\sum_v t \dot{m}_{\text{prod},v}} \quad (2)$$

The capital expenditures $CAPEX$ according to Eq. (3) are composed of investment costs for the system C_{sys} and costs for the heat exchanger network according to Yee & Grossmann [23].

$$\begin{aligned}
 CAPEX = AF_{\text{inv}} & \left[\underbrace{C_{\text{sys}}}_{\text{investment costs}} + \underbrace{\sum_i \sum_j \sum_k c_{v,\text{hex}} \left(\frac{q_{ijk}}{U_{ij} LMTD_{ijk}} \right)^\beta}_{\text{variable HEX stream costs}} \right. \\
 & + \underbrace{\sum_i c_{v,\text{hex}} \left(\frac{q_{cu,i}}{U_{cu,i} LMTD_{cu,i}} \right)^\beta}_{\text{variable HEX cold utility costs}} + \underbrace{\sum_j c_{v,\text{hex}} \left(\frac{q_{hu,j}}{U_{hu,j} LMTD_{hu,j}} \right)^\beta}_{\text{variable HEX hot utility costs}} \\
 & \left. + \underbrace{\sum_i \sum_j \sum_k c_{f,\text{hex}} z_{ijk} + \sum_i c_{f,\text{hex}} z_{cu,i} + \sum_j c_{f,\text{hex}} z_{hu,j}}_{\text{fixed investment costs hex}} \right] \quad (3)
 \end{aligned}$$

The operating expenditures $OPEX$ according to Eq. (4) are composed of feedstock and electricity costs depending on the annual full load hours t .

$$OPEX = AF_{\text{op}} t \left[\underbrace{c_{\text{CO}_2} \dot{m}_{\text{CO}_2} + c_{\text{H}_2\text{O}} \dot{m}_{\text{H}_2\text{O}} + c_{\text{air}} \dot{m}_{\text{air}}}_{\text{feedstock costs}} + \underbrace{c_{\text{el}} \left(P_{\text{sys}} + \sum_j \epsilon_{\text{uh}} q_{\text{uh},j} + \sum_i \epsilon_{\text{uc}} q_{\text{uc},i} \right)}_{\text{electricity costs}} \right] \quad (4)$$

In our model, CAPEX and OPEX are interrelated and impact the overall production costs of synthetic fuels. A higher CAPEX can lead to more efficient systems that reduce OPEX. For example, investing in a more efficient heat exchanger network can decrease energy consumption, thereby reducing electricity costs, which are a significant component of OPEX.

However, this relationship is not linear and requires careful optimization to ensure economic viability. The multi-criteria optimization approach allows us to balance these competing factors. By considering both PtL-efficiency and fuel production costs, we can identify designs that do not overly sacrifice economic performance for efficiency gains. This holistic approach ensures that the optimized system remains cost-effective while achieving high efficiency, ultimately leading to sustainable and economically viable synthetic fuel production.

3.2. Cost parameters

The coupled optimization of the PtL-plant is performed with initial values for electricity and CO_2 costs based on current market conditions. Fig. 2 shows the chosen domain of cost parameters. The production of synthetic fuels can only be climate neutral if only CO_2 -neutral produced electricity is used. For a location in central Europe and electricity production from wind and solar PV, Janssen et al. [28] suggest a price of $c_{\text{el,base}} = 20 \text{ €/MWh}$. For the lower electricity price limit $c_{\text{el,min}}$, we refer to Sens et al. [29] where in 2050, electricity from PV and wind onshore can be expected to have a levelized cost of electricity (LCOE) of approximately 10 €/MWh . We consider this as a best-case scenario for future electricity price developments. The upper limit of $c_{\text{el,max}} = 100 \text{ €/MWh}$ is derived from the LCOE for wind offshore in 2050 [29].

The price for emitted CO_2 can be levied either with a cap-and-trade system like the Emission Trading System (ETS) or as a carbon tax [30]. Both policies aim to have the government financially penalize greenhouse gas emissions and thus force the polluters to reduce. What CO_2 pricing will look like for synthetic fuels has not yet been defined. In any case, it can be assumed that the end users will bear the costs. In this paper, we use a CO_2 price of $c_{\text{CO}_2,\text{base}} = 50 \text{ €/t}$ as a base value. This corresponds roughly to the average CO_2 tax in Europe according to the Carbon Pricing Dashboard of The World Bank [31]. A minimum price of $c_{\text{CO}_2,\text{min}} = 0 \text{ €/t}$ is assumed as an economic best-case scenario. This scenario represents sites with no CO_2 pricing or where special regulations for synthetic fuels have been enacted. As a maximum value, a CO_2 price of $c_{\text{CO}_2,\text{min}} = 150 \text{ €/t}$ is assumed. This represents a roadmap for realistic price development towards 2050 [32–34].

3.3. Implementation

The optimization problem was formulated with Yalmip R20210331 [35] and Matlab R2022b [36]. Gurobi 10.0.0 was used as MILP solver [37]. A MIP gap of less than 1% was set as a termination criterion for the optimization. All computations were performed on a 64-core server (AMD EPYC 7702P) with 265 GB of RAM.

All non-linearities are piecewise linearly approximated, analogous to the approach from Huber et al. [20]. A root-mean-square error (RMSE) of less than 1% is set as a termination criterion for the refinement of the approximations.

All cost parameters are given in Appendix C.

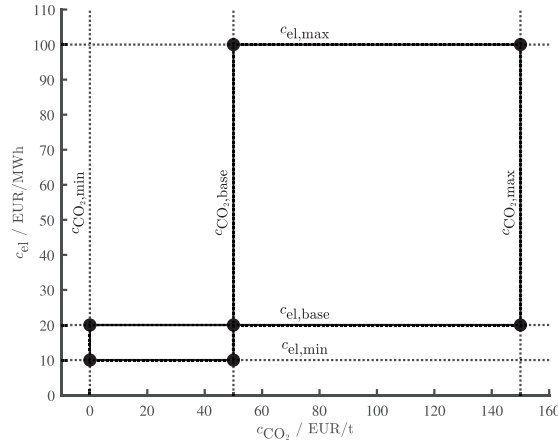


Fig. 2. Upper and lower limits of the cost parameters for electricity c_{el} and CO_2 c_{CO_2} .

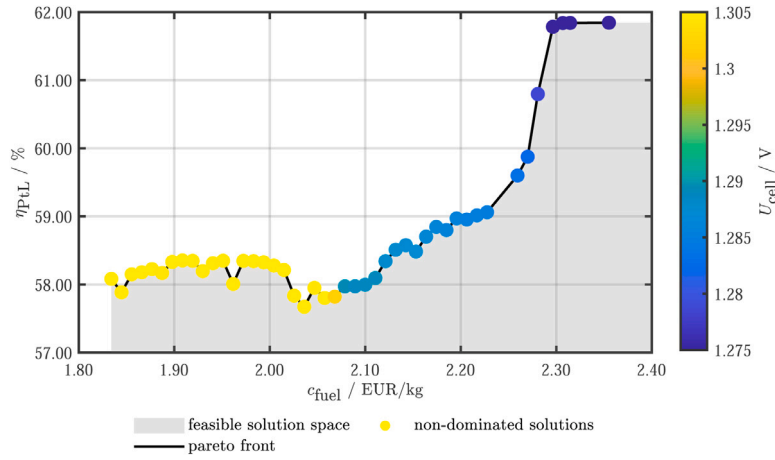


Fig. 3. Non-dominated solutions and Pareto front of the coupled optimization. The color coding represents the cell voltage as the main operating parameter.

4. Results

The non-dominated solutions of the antagonistic objectives are illustrated as a Pareto front in Fig. 3. The non-dominated solutions represent the trade-off on fuel production costs and PtL-efficiency at an electricity price of $c_{el,base} = 20 \text{ €/MWh}$ and a CO_2 price of $c_{CO_2,base} = 50 \text{ €/t}$. The resulting HENs at the extreme values at a cell voltage of $U_{cell} = 1.275 \text{ V}$ and $U_{cell} = 1.305 \text{ V}$ are shown in Appendix D. The color coding represents the cell voltage as the critical operating parameter. The slight scattering of the Pareto front at low production costs results from the solver time out and the optimality gap of the solution. There were no solutions found for the gaps around high production costs within the defined solver time. The stream plots at the corner points of the Pareto front and the characteristic values such as number the of heat exchangers, power of the utilities and the costs can be obtained from [20].

An essential aspect of the Pareto front is that the production costs increase with decreasing cell voltage. Further, the shape of the Pareto front allows us to derive the impact of design and operating parameters. At the highest cell voltage of $U_{cell} = 1.305 \text{ V}$, the PtL-efficiency remains almost unchanged between 57.67% and 58.35%. The production costs, however, vary from 1.83 €/kg to 2.06 €/kg. This indicates that design parameters significantly influence production costs but only barely the efficiency in this region. Conversely, at the upper production cost range, the influence of the cell voltage dominates. The production costs remain almost constant while the PtL-efficiency increases significantly.

Price changes are analyzed based on the non-dominated solutions optimized with initial cost parameters. Production costs are recalculated for each solution at constant PtL-efficiencies. This is feasible because the cost parameters for CO_2 and electricity occur as linear terms only in the objective function of the production costs and not in that of the PtL-efficiency; see Eq. (2) and (4), respectively. Thus, only the production costs change depending on the cost parameters, while the PtL-efficiency remains unchanged.

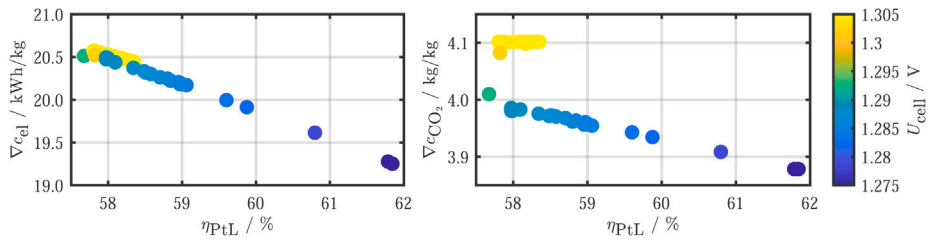


Fig. 4. Calculated sensitivities for electricity and CO₂ price changes as a function of PtL-efficiency.

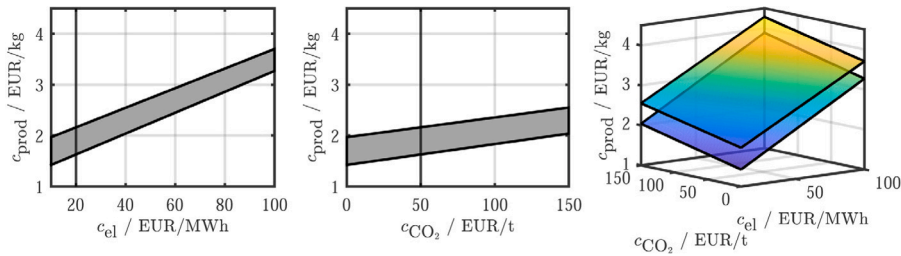


Fig. 5. Upper and lower production costs as a function of electricity and CO₂ price. Left: Isolated impact of electricity price. Middle: Isolated impact of the CO₂ price. Right: Combined impact.

We quantify the impact of the cost parameters with the help of the parameter sensitivity defined by Eqs. (5) and (6).

$$\nabla c_{el} = AF_{op} \frac{\left[P_{sys} + \left(\sum_j \epsilon_{uh} q_{uh,j} + \sum_i \epsilon_{uc} q_{uc,i} \right) \right]}{\sum_v \dot{m}_{prod,v}} \quad (5)$$

$$\nabla c_{CO_2} = AF_{op} \frac{\dot{m}_{CO_2}}{\sum_v \dot{m}_{prod,v}} \quad (6)$$

Fig. 4 on the left shows the sensitivities to electricity price changes. With an annualization factor of $AF_{op} = 1$, ∇c_{el} can be interpreted as energy consumption to produce 1 kg of synthetic fuel, respectively FT-wax, diesel and naptha. Fasihi et al. obtained a slightly higher value of 21.98 kWh/kg for a similar PtL-plant with an ambient air scrubber, reverse water gas shift reaction (RWGS) and alkaline electrolysis cell [38]. In our case, PtL-efficiency strongly correlates with the sensitivity. Higher efficiencies are, therefore, less susceptible to price changes.

The sensitivities to CO₂ price changes are shown in Fig. 4 on the right. They can be interpreted as the utilized amount of CO₂ per kg of synthetic fuel produced. The process presented by Fasani et al. [38] requires 3.20 kg/kg. In this case, the sensitivity correlates less strongly with the efficiency but instead much more with the cell voltage. Therefore, plant designs with low cell voltages are less susceptible to price changes.

Based on the sensitivities, we calculated the production costs for each non-dominated solution as function of the electricity and CO₂ prices. Fig. 5 shows the highest and lowest production costs. The minimum and maximum production costs are shown as a function of electricity prices on the left and CO₂ prices on the right. The vertical lines show the current cost parameters $c_{el,base}$ and $c_{CO_2,base}$ from Fig. 2. The minimum and maximum production costs are shown for both cost parameters on the right side of Fig. 5. All non-dominated solutions are between these two planes. In this context, the sensitivities can be interpreted as slopes of the limiting lines, respectively, planes. Accordingly, the higher the sensitivity, the more sensitive the solution reacts to price changes. It can be concluded from the plane slopes that the influence of the electricity price on the production costs is about five times larger than that of the CO₂ price.

The price changes affect the shape of the Pareto front depending on the efficiency. On the top of Fig. 6, three Pareto fronts for minimum, initial and maximum electricity prices are shown. Electricity prices have a substantial effect on production costs. When electricity costs are high, it is noticeable that the Pareto front forms a pocket in the efficiency range from 59.0% to 61.8%. If higher electricity costs are expected, selecting a plant design with these parameters should be avoided since lower production costs can be expected at higher and lower efficiencies. The Pareto fronts for different CO₂ prices in Fig. 6 on the bottom do not create pockets. It is noticeable that the influence on the production costs is significantly lower.

Fig. 7 shows the collective impact of price changes. For each extreme value, a Pareto front is shown. It should be noted that the lines for $c_{CO_2,min}$ and $c_{el,min}$ overlap almost completely. If the electricity price is reduced to 10 €/MW and the CO₂ price is dropped to 0, synthetic fuels can be produced in the 1.42 €/kg to 1.97 €/kg range. Compared to the current market price for gasoline of about 0.5 €/kg, the large-scale introduction of synthetic fuels will be an economic challenge [39]. At the highest electricity and CO₂ prices of 100 €/MW and 150 €/t, the production costs range from 3.88 €/kg to 4.28 €/kg. Whether synthetic fuels will prevail at this price level is questionable.

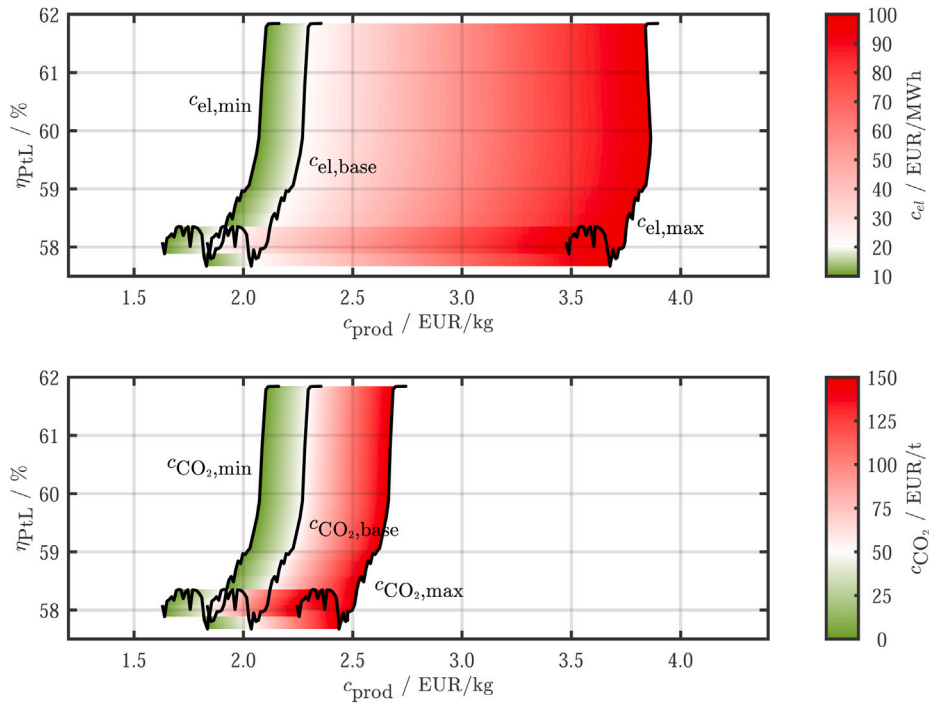


Fig. 6. Pareto fronts for changing electricity prices (top) and CO₂ prices (bottom). The color gradient represents the shift of the Pareto front due to price changes.

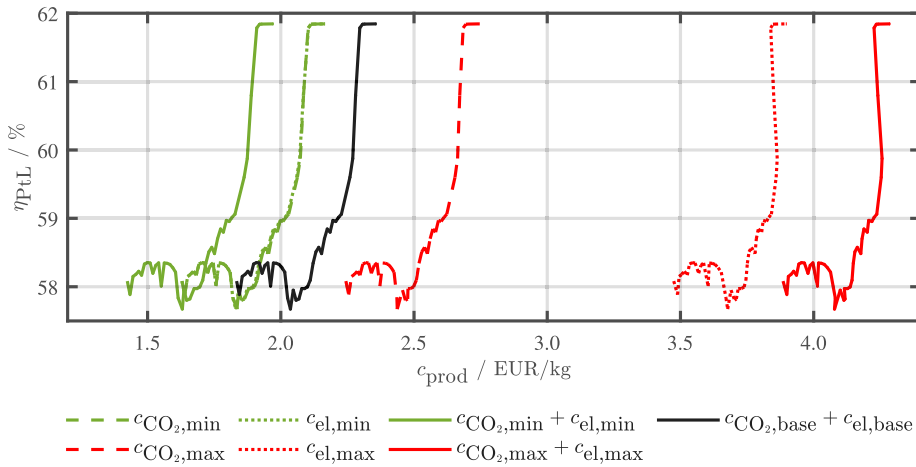


Fig. 7. Pareto fronts for the extreme values of the cost parameters: Initial costs (black), cost reduction (green), cost increase (red).

5. Conclusion

In this paper, we investigated the impact of changing electricity and CO₂ prices on the production costs of synthetic fuels. A novel 1 MW PtL-plant was considered as a use case. The main components were modeled and the cell voltage of the co-SOEC was optimized as a crucial operating parameter coupled with the heat exchanger network and the internal heat supply as design parameters. A formulation for PtL-efficiency and production cost was presented as objective functions. Based on the optimization results, the sensitivities for electricity and CO₂ price changes were calculated and their correlation with the design and operational

parameters was discussed. A comprehensive cost analysis was performed with defined scenarios for decreasing and increasing cost parameters.

Our results show that the non-dominated solutions of the Pareto front in the low-efficiency area depend more on the design parameters than on the cell voltage of the co-SOEC as the operating parameter. On the other hand, a distinct dependence on the cell voltage can be seen in the high-efficiency area. Current electricity and CO₂ prices results in production costs in the range of 1.83–2.36 €/kg and a PtL-efficiency of 57.67–61.84%. Further, we were able to show that the influence of the electricity price is about five times larger than that of the CO₂ price. The sensitivity of the electricity price correlates strongly inversely with the efficiency. This implies that higher efficiencies are less affected by price increases. Substantial price increases lead to pockets in the Pareto front, which may preclude specific design and operating areas. A further key outcome is that our results allow us to estimate the expected production costs depending on price changes. In the economic best-case scenario, production costs can be reduced to the range of 1.42–1.97 €/kg. In the worst-case scenario, production costs increase up to 3.88–4.28 €/kg.

In this study, we focused on a smaller-scale plant to explore the technical and economic feasibility of the proposed synthetic fuel production pathway. This scale allowed for a detailed analysis of technological parameters and optimization processes, while effectively managing risks and investments. Although larger plants could benefit from economies of scale and achieve lower production costs, the insights gained from the investigation at this smaller scale are crucial. These findings provide valuable information necessary for designing and developing more economically viable, large-scale systems. We further provided an overview of current production costs and the influence of design and operating parameters on future cost developments. A central and, above all, necessary basis for decision-making has been developed with this paper. It enables the decision-makers to evaluate the design and its consequences for sustainable synthetic fuel production. With this paper, we promote the efficient and cost-effective production of synthetic fuels and contribute significantly to a climate-neutral and sustainable future.

Funding

This research was funded by the Austrian Research Promotion Agency (FFG) under grant number 884340 and TU Wien Bibliothek through its Open Access Funding Programme.

CRediT authorship contribution statement

David Huber: Writing – review & editing, Writing – original draft, Visualization, Validation, Supervision, Software, Resources, Methodology, Investigation, Formal analysis, Data curation, Conceptualization. **Felix Birkelbach:** Writing – review & editing, Project administration, Investigation, Conceptualization. **René Hofmann:** Writing – review & editing, Project administration, Funding acquisition.

Declaration of competing interest

The authors declare the following financial interests/personal relationships which may be considered as potential competing interests: Rene Hofmann reports financial support was provided by Austrian Research Promotion Agency. David Huber reports financial support was provided by TU Wien Library. If there are other authors, they declare that they have no known competing financial interests or personal relationships that could have appeared to influence the work reported in this paper.

Data availability

No data was used for the research described in the article.

Appendix A. Product properties

Table A.1 lists the chemical and physical product parameters. These are invariant for the system regardless of the cell voltage.

Table A.1

Chemical and physical product properties at 40 °C and 101 324.97 Pa downstream the upgrading.
Source: Adapted from [20].

v	Product	$h_{\text{prod}}/\text{MJ/kg}$	$\rho_{\text{prod}}/\text{kg/m}^3$	$\mu_{\text{prod}}/\text{mPa/s}$
1	FT-wax	43.887	797.73	6.7477
2	diesel	44.345	748.81	1.5983
3	naphtha	44.676	516.17	0.5893

Table B.2

Stream data with limits for inlet, outlet temperature and flow capacity.

Source: Adapted from [20].

Stream	$T^{\text{in}}/^{\circ}\text{C}$	$T^{\text{out}}/^{\circ}\text{C}$	$F/\text{kW/K}$
H1	40.0	35.0	[1.71, 2.16]
H2	[127.9, 131.1]	[34.0, 35.0]	[0.09, 0.12]
H3	[169.8, 174.1]	[34.0, 35.0]	[0.09, 0.12]
H4	210.0	190.0	[0.27, 0.28]
H5	190.0	120.0	[0.56, 0.58]
H6	120.0	30.0	[0.48, 0.50]
H7	[45.4, 57.0]	31.0	[2.35, 2.95]
H8	138.9	137.9	[59.60, 94.40]
H9	[805.2, 825.5]	[34.0, 35.0]	[0.10, 0.13]
H10	[49.5, 50.7]	[34.0, 35.0]	[0.65, 0.88]
H11	101.8	30.0	[0.51, 0.64]
H12	190.0	188.0	[76.88, 80.45]
C1	[318.0, 319.2]	[825.0, 870.5]	[0.14, 0.18]
C2	116.9	124.2	[20.02, 25.12]
C3	[57.3, 58.8]	825.0	[0.25, 0.33]
C4	137.9	139.9	[105.77, 142.64]
C5	138.9	[426.6, 449.4]	[0.10, 0.11]
C6	35.0	[115.9, 145.4]	[0.05, 0.06]
C7	20.3	[189.5, 199.6]	[0.15, 0.21]
CS1	900.0	[100, 890]	[59.60, 94.40]
CS2	900.0	[100, 890]	[0.10, 0.13]
CS3	900.0	[100, 890]	[0.65, 0.88]

Appendix B. Stream data

Table B.2 provides the stream parameters or their bounds. Values without brackets are independent of the cell voltage constant. Values in square brackets are bounds of stream parameters dependent on cell voltage. The heat transfer coefficients are $U = 0.5 \text{ kW}/(\text{m}^2 \text{ K})$ for all streams.

The HEN problem has been modeled with $N_{\text{st}} = 3$ stages for the heat exchange. The minimum temperature difference of $\Delta T_{\text{min}} = 1 \text{ K}$ must not be exceeded.

Appendix C. Cost parameters

Table C.3

Cost parameters and their source.

Source: Adapted from [20].

Cost share	Value	Comment/source
β	0.8	
$c_{\text{f,hex}}$	1013.6 €/y	AISI 316, interpolated from [40]
$c_{\text{v,hex}}$	61.8 €/m ² y	
C_{sys}	10 000 000 €	project internal estimation & [41]
$c_{\text{H}_2\text{O}}$	3.54 €/t	mean for Europe [42]
$c_{\text{CO}_2, \text{base}}$	50 €/t	average CO ₂ tax in Europe [31]
c_{air}	0 €/t	ambient air is free of charge
$c_{\text{el,base}}$	20 €/MWh	at a projected plant location in Europe [28]

Table C.3 lists the cost parameters and their sources. The investment costs are depreciated linearly over a period of 20 years. Thus, the annual depreciation factor is $AF_{\text{inv}} = 1/20\text{y}$. The depreciation factor for the operating costs is assumed to be $AF_{\text{op}} = 1/\text{y}$. Analogous to [13,41,43], $t = 8000 \text{ h/y}$ full load operating hours per year are assumed.

Appendix D. Stream plots

The points on the Pareto front represent different HEN configurations. Figs. D.8 and D.9 show the HEN configurations at the extreme points at a cell voltage of $U_{\text{cell}} = 1.275 \text{ V}$ and $U_{\text{cell}} = 1.305 \text{ V}$ respectively.

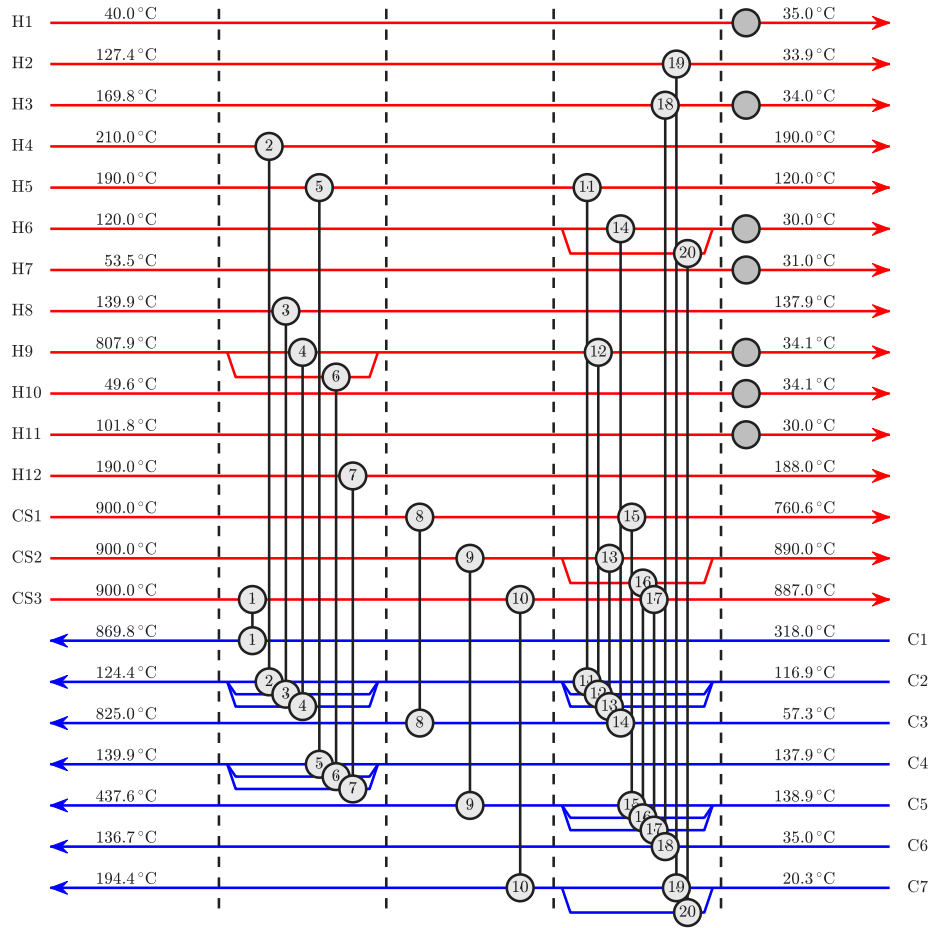


Fig. D.8. Stream plot with 27 heat exchangers resulting from the simultaneous optimization. Characteristic figures: $\eta_{\text{PtL}} = 61.84\%$, $c_{\text{prod}} = 2.36 \text{ €/kg}$, $U_{\text{cell}} = 1.275 \text{ V}$. Source: Adapted from Huber et al. [20].

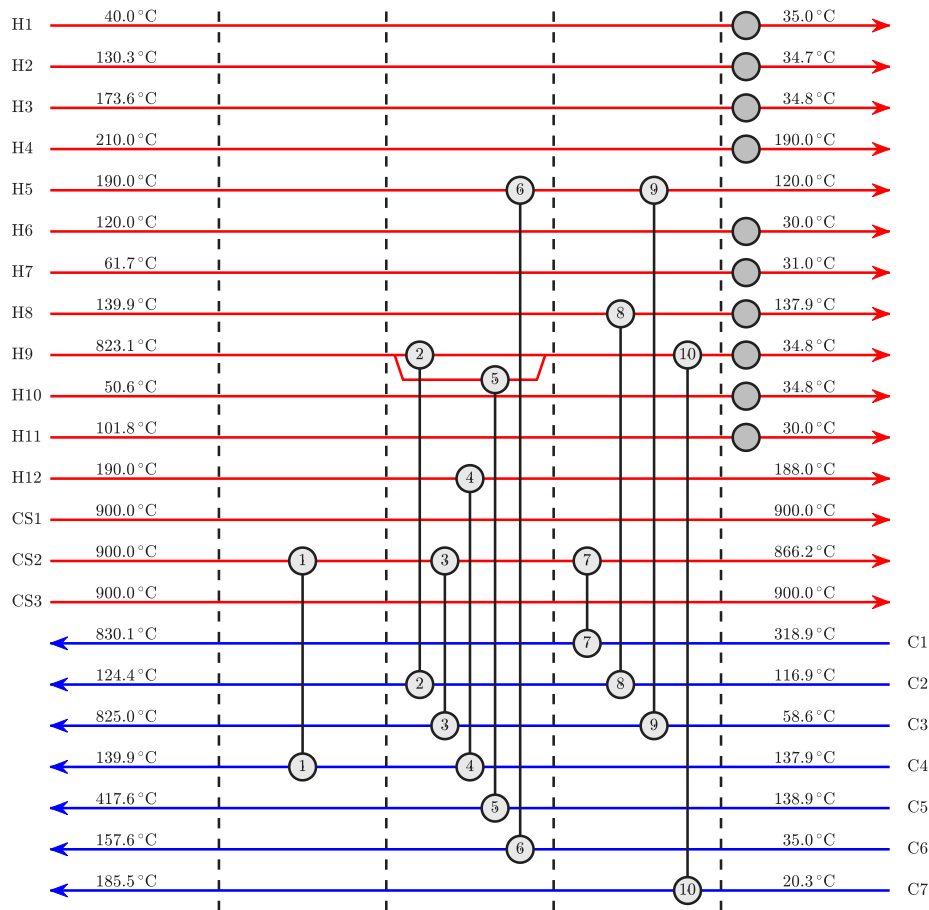


Fig. D.9. Stream plot with 20 heat exchangers resulting from the simultaneous optimization. Characteristic figures: $\eta_{\text{ptL}} = 58.08\%$, $c_{\text{prod}} = 1.83 \text{ €/kg}$, $U_{\text{cell}} = 1.305 \text{ V}$. Source: Adapted from Huber et al. [20].

References

- [1] International Energy Agency, CO2 Emissions in 2022, Technical Report, 2022, URL: <https://www.iea.org/reports/co2-emissions-in-2022>.
- [2] International Energy Agency, Global CO2 Emissions from Transport by Sub-Sector in the Net Zero Scenario, Technical Report, 2022, URL: <https://www.iea.org/energy-system/transport>.
- [3] F. Ueckerdt, C. Bauer, A. Dirnmaier, J. Everall, R. Sacchi, G. Luderer, Potential and risks of hydrogen-based e-fuels in climate change mitigation, *Nature Clim. Change* 11 (5) (2021) 384–393, <http://dx.doi.org/10.1038/s41558-021-01032-7>, Number: 5 Publisher: Nature Publishing Group.
- [4] G. Gahleitner, Hydrogen from renewable electricity: An international review of power-to-gas pilot plants for stationary applications, *Int. J. Hydrog. Energy* 38 (5) (2013) 2039–2061, <http://dx.doi.org/10.1016/j.ijhydene.2012.12.010>, URL: <https://linkinghub.elsevier.com/retrieve/pii/S0360319912026481>.
- [5] S. Pratschner, M. Hammerschmid, S. Müller, F. Winter, Evaluation of CO2 sources for power-to-liquid plants producing Fischer-Tropsch products, *J. CO2 Util.* 72 (2023) 102508, <http://dx.doi.org/10.1016/j.jcou.2023.102508>.
- [6] eFuel Alliance e.V., eFuel Produktionskarte, 2023, URL: <https://www.efuel-alliance.eu/de/efuels/efuel-produktionskarte>.
- [7] Fraunhofer IEE, Global PtX Atlas 1.2.1 (Januar 2023), 2023, URL: <https://maps.iee.fraunhofer.de/ptx-atlas/>.
- [8] Siemens energy, Haru Oni: Base camp of the future, 2023, URL: <https://www.siemens-energy.com/global/en/news/magazine/2022/haru-oni.html>.
- [9] T. Ngan Do, C. You, J. Kim, A CO2 utilization framework for liquid fuels and chemical production: Techno-economic and environmental analysis, *Energy Environ. Sci.* 15 (1) (2022) 169–184, <http://dx.doi.org/10.1039/D1EE01444G>, Publisher: Royal Society of Chemistry.
- [10] S. Brynolf, M. Taljegård, M. Grahn, J. Hansson, Electrofuels for the transport sector: A review of production costs, *Renew. Sustain. Energy Rev.* 81 (2018) 1887–1905, <http://dx.doi.org/10.1016/j.rser.2017.05.288>.
- [11] A.R. Dahiru, A. Vuokila, M. Huuhtanen, Recent development in Power-to-X: Part I - A review on techno-economic analysis, *J. Energy Storage* 56 (2022) 105861, <http://dx.doi.org/10.1016/j.est.2022.105861>.
- [12] M. Götz, J. Lefebvre, F. Mörs, A. McDaniel Koch, F. Graf, S. Bajohr, R. Reimert, T. Kolb, Renewable Power-to-Gas: A technological and economic review, *Renew. Energy* 85 (2016) 1371–1390, <http://dx.doi.org/10.1016/j.renene.2015.07.066>.
- [13] V. Dieterich, A. Buttler, A. Hanel, H. Splithoff, S. Fendt, Power-to-liquid via synthesis of methanol, DME or Fischer-Tropsch-fuels: A review, *Energy Environ. Sci.* 13 (10) (2020) 3207–3252, <http://dx.doi.org/10.1039/D0EE01187H>.
- [14] C. Graves, S.D. Ebbesen, M. Mogensen, K.S. Lackner, Sustainable hydrocarbon fuels by recycling CO2 and H2O with renewable or nuclear energy, *Renew. Sustain. Energy Rev.* 15 (1) (2011) 1–23, <http://dx.doi.org/10.1016/j.rser.2010.07.014>.
- [15] A. Tremel, P. Wasserscheid, M. Baldauf, T. Hammer, Techno-economic analysis for the synthesis of liquid and gaseous fuels based on hydrogen production via electrolysis, *Int. J. Hydrog. Energy* 40 (35) (2015) 11457–11464, <http://dx.doi.org/10.1016/j.ijhydene.2015.01.097>.

- [16] D. Leeson, P. Fennell, N. Shah, C. Petit, N.M. Dowell, A techno-economic analysis and systematic review of carbon capture and storage (CCS) applied to the iron and steel, cement, oil refining and pulp and paper industries, *Energy Procedia* 114 (2017) 6297–6302, <http://dx.doi.org/10.1016/j.egypro.2017.03.1766>.
- [17] A. Sternberg, A. Bardow, Power-to-What? – Environmental assessment of energy storage systems, *Energy Environ. Sci.* 8 (2) (2015) 389–400, <http://dx.doi.org/10.1039/C4EE03051F>.
- [18] S. Michailos, M. Walker, A. Moody, D. Poggio, M. Pourkashanian, A techno-economic assessment of implementing power-to-gas systems based on biomethanation in an operating waste water treatment plant, *J. Environ. Chem. Eng.* 9 (1) (2021) 104735, <http://dx.doi.org/10.1016/j.jece.2020.104735>.
- [19] M. Mahrach, G. Miranda, C. León, E. Segredo, Comparison between single and multi-objective evolutionary algorithms to solve the knapsack problem and the travelling salesman problem, *Mathematics* 8 (11) (2020) 2018, <http://dx.doi.org/10.3390/math8112018>.
- [20] D. Huber, F. Birkelbach, R. Hofmann, Unlocking the potential of synthetic fuel production: Coupled optimization of heat exchanger network and operating parameters of a 1 MW power-to-liquid plant, *Chem. Eng. Sci.* (2023) 119506, <http://dx.doi.org/10.1016/j.ces.2023.119506>.
- [21] D. Huber, K. Werding, F. Birkelbach, R. Hofmann, Highly efficient heat integration of a power-to-liquid process using MILP, in: *36th International Conference on Efficiency, Cost, Optimization, Simulation and Environmental Impact of Energy Systems (ECOS 2023)*, vol. I, part A-I, ULPGC, Las Palmas De Gran Canaria, Spain, 2023, pp. 1513–1523.
- [22] D. Huber, F. Birkelbach, R. Hofmann, HENS unchained: MILP implementation of multi-stage utilities with stream splits, variable temperatures and flow capacities, *Energies* 16 (12) (2023) 4732, <http://dx.doi.org/10.3390/en16124732>.
- [23] T.F. Yee, I.E. Grossmann, Simultaneous optimization models for heat integration—II. Heat exchanger network synthesis, *Comput. Chem. Eng.* 14 (10) (1990) 1165–1184, [http://dx.doi.org/10.1016/0098-1354\(90\)85010-8](http://dx.doi.org/10.1016/0098-1354(90)85010-8).
- [24] D.R. Lewin, H. Wang, O. Shalev, A generalized method for HEN synthesis using stochastic optimization – I. General framework and MER optimal synthesis, *Comput. Chem. Eng.* 22 (10) (1998) 1503–1513, [http://dx.doi.org/10.1016/S0098-1354\(98\)00220-8](http://dx.doi.org/10.1016/S0098-1354(98)00220-8).
- [25] X. Luo, Q.-Y. Wen, G. Fieg, A hybrid genetic algorithm for synthesis of heat exchanger networks, *Comput. Chem. Eng.* 33 (6) (2009) 1169–1181, <http://dx.doi.org/10.1016/j.compchemeng.2008.12.003>.
- [26] J.A. Stampfli, B.H. Ong, D.G. Olsen, B. Wellig, R. Hofmann, Applied heat exchanger network retrofit for multi-period processes in industry: A hybrid evolutionary algorithm, *Comput. Chem. Eng.* 161 (2022) 107771, <http://dx.doi.org/10.1016/j.compchemeng.2022.107771>.
- [27] J.P. Vielma, G.L. Nemhauser, Modeling disjunctive constraints with a logarithmic number of binary variables and constraints, *Math. Program.* 128 (1) (2011) 49–72, <http://dx.doi.org/10.1007/s10107-009-0295-4>.
- [28] J. Janssen, M. Weeda, R.J. Detz, B. van der Zwaan, Country-specific cost projections for renewable hydrogen production through off-grid electricity systems, *Appl. Energy* 309 (2022) 118398, <http://dx.doi.org/10.1016/j.apenergy.2021.118398>.
- [29] L. Sens, U. Neuling, M. Kaltschmitt, Capital expenditure and levelized cost of electricity of photovoltaic plants and wind turbines – Development by 2050, *Renew. Energy* 185 (2022) 525–537, <http://dx.doi.org/10.1016/j.renene.2021.12.042>.
- [30] P.K. Kruse-Andersen, P.B. Sørensen, Optimal carbon taxation in EU frontrunner countries: Coordinating with the EU ETS and addressing leakage, *Climate Policy* (2022) 1–13, <http://dx.doi.org/10.1080/14693062.2022.2145259>.
- [31] The World Bank, Carbon pricing dashboard, 2023, URL: https://carbonpricingdashboard.worldbank.org/map_data.
- [32] BloombergNEF, Carbon offset prices could increase fifty-fold by 2050, 2023, URL: <https://about.bnef.com/blog/carbon-offset-prices-could-increase-fifty-fold-by-2050/>.
- [33] Essential, Expensive and Evolving: the Outlook for Carbon Credits and Offsets, Technical Report, EY Net Zero Centre, Sydney, 2022.
- [34] GHG Market Sentiment Survey 2022, Technical Report, IETA, 2022, URL: <https://www.ieta.org/resources/Documents/IETA%20GHG%20Market%20Sentiment%20Survey%20Report%202022.pdf>.
- [35] J. Löfberg, A toolbox for modeling and optimization in MATLAB, in: *Proceedings of the CACSD Conference*, 2004, p. 289, <http://dx.doi.org/10.1109/CACSD.2004.1393890>.
- [36] The MathWorks Inc., MATLAB version: 9.13.0 (R2022b), 2022, Natick, Massachusetts, United States, URL: <https://www.mathworks.com>.
- [37] Gurobi Optimization, LLC, Gurobi optimizer reference manual, 2023, URL: <https://www.gurobi.com>.
- [38] M. Fasihi, D. Bogdanov, C. Breyer, Techno-economic assessment of Power-to-Liquids (PtL) fuels production and global trading based on hybrid PV-Wind power plants, *Energy Procedia* 99 (2016) 243–268, <http://dx.doi.org/10.1016/j.egypro.2016.10.115>.
- [39] U.S. Energy Information Administration, U.S. total gasoline wholesale/resale price by refiners (dollars per gallon), 2023, URL: <https://www.eia.gov/petroleum/data.php>.
- [40] DACE Price Booklet: Cost Information for Estimation and Comparison, Edition 35, DACE Cost and Value, Nijkerk, 2021, OCLC 1303572720.
- [41] G. Herz, C. Rix, E. Jacobasch, N. Müller, E. Reichelt, M. Jahn, A. Michaelis, Economic assessment of Power-to-Liquid processes – Influence of electrolysis technology and operating conditions, *Appl. Energy* 292 (2021) 116655, <http://dx.doi.org/10.1016/j.apenergy.2021.116655>.
- [42] EurEau, Europe's Water in Figures: An Overview of the European Drinking Water and Waste Water Sectors, 2021, URL: <https://www.eureau.org/resources/publications/eureau-publications/5824-europe-s-water-in-figures-2021/file>.
- [43] S. Adelung, Global sensitivity and uncertainty analysis of a Fischer-Tropsch based power-to-liquid process, *J. CO₂ Util.* 65 (2022) 102171, <http://dx.doi.org/10.1016/j.jcou.2022.102171>.